PHYSICAL REVIEW B **81**, 125432 (2010)

Normal-incidence x-ray standing-wave determination of the adsorption geometry of PTCDA on Ag(111): Comparison of the ordered room-temperature and disordered low-temperature phases

A. Hauschild,[1] R. Temirov,[2,3,*] S. Soubatch,[2,3,*] O. Bauer,[1] A. Schöll,[4] B. C. C. Cowie,[5] T.-L. Lee,[5] F. S. Tautz,[2,3,*] and M. Sokolowski[1,†]

[1]*Institut für Physikalische und Theoretische Chemie der Universität Bonn, Wegelerstraße 12, 53115 Bonn, Germany*
[2]*Institut für Bio- und Nanosysteme 3, Forschungszentrum Jülich, 52425 Jülich, Germany*
[3]*Fundamentals of Future Information Technology, Jülich Aachen Research Alliance (JARA-FIT), Forschungszentrum Jülich GmbH, 52425 Jülich, Germany*
[4]*Experimentelle Physik II, Am Hubland, Universität Würzburg, 97074 Würzburg, Germany*
[5]*European Synchrotron Radiation Facility, Boîte Postale 220, 38043 Grenoble Cedex, France*

(Received 7 September 2009; revised manuscript received 24 February 2010; published 26 March 2010)

Normal incidence x-ray standing wave (NIXSW) experiments have been performed for monolayers of 3,4,9,10-perylene-tetracarboxylic-dianhydride (PTCDA) adsorbed on the Ag(111) surface. Two phases were analyzed: the low-temperature phase (LT phase), which is disordered and obtained for deposition at substrate temperatures below 150 K, and the ordered phase, which is obtained for deposition at room temperature (RT phase). From the NIXSW analysis the vertical bonding distances to the Ag surface were obtained for the averaged carbon atoms and the two types of chemically different oxygen atoms in the terminal anhydride groups. For the LT phase, we find about 2% (0.05 Å) and 8% (0.21 Å) smaller averaged bonding distances for the C and O atoms, respectively, compared to the RT phase. In both phases, the planar geometry of the free molecule is distorted; in particular, the carboxylic O atoms are closer to the surface by 0.20 Å (RT) and 0.31 Å (LT) with respect to the averaged C distance. The difference between the vertical bonding distances of the carboxylic and anhydride O atoms is found to be 0.32 (RT) and 0.33 Å (LT). These structural parameters of the two phases are compared to those of PTCDA monolayers adsorbed on Au(111) and Cu(111) surfaces and are discussed in the frame of current bonding models.

DOI: 10.1103/PhysRevB.81.125432 PACS number(s): 68.43.Fg, 82.65.+r, 79.60.Dp

I. INTRODUCTION

Presently there exists a large interest in the exact determination of the adsorption geometry of large π-conjugated organic molecules on surfaces because (a) this information is essential for the understanding of the growth behavior and properties of semiconducting organic films on surfaces[1] and (b) since theoretical calculations of larger molecules on surfaces have recently become possible[2–5] and ask for quantitative geometric parameters to test their predictive power.

Here we report details of a normal incidence x-ray standing wave (NIXSW) analysis of the prototype molecule 3,4,9,10-perylene-tetracarboxylic-dianhydride (PTCDA, see Fig. 6, below) adsorbed on the Ag(111) surface for the ordered room-temperature (RT) and disordered low-temperature (LT) phases. The geometric parameters of this analysis have been reported in two short articles before (see Refs. 6 and 7 and comments in Refs. 8 and 9). Here we give the original experimental data and describe the details of the analysis. In addition we discuss our finding in relation to recently published bonding distances of PTCDA on other (111)-fcc surfaces. For a recent review on the adsorption of PTCDA on noble metal surfaces see Ref. 10.

The NIXSW method is highly attractive for the determination of vertical bonding heights of organic molecules on surfaces for a number of reasons: (i) for many cases the evaluation does not require a structural model of the adsorbate, (ii) the method is not limited by the size of the molecules, as for instance low-energy electron diffraction, and specific signal atoms may be selected by photoemission, and (iii) it is possible to gain further intramolecular information, whenever the photoelectrons from chemically nonequivalent atoms of one element can be distinguished. Roughly speaking, the NIXSW method determines atomic positions relative to a standing x-ray wave field generated by the substrate Bragg planes by measuring their photoelectron or Auger yield. Details of the NIXSW technique can be found in several reviews.[11–14] Over the last years the adsorption geometries of a number of π-conjugated, mainly planar molecules adsorbed on (111)-fcc surfaces have been investigated by NIXSW.[15–19] For PTCDA, NIXSW measurements were, besides on Ag(111), performed on Au(111) (Ref. 20) and Cu(111),[21] and first trends between the anticipated strength of the interfacial interaction and the bonding geometry become visible.

Briefly summarizing, PTCDA crystallizes in a long-range ordered commensurate herringbone monolayer structure on Ag(111) when deposited at RT.[22,23] The molecules are in a planar adsorption geometry with two molecules within the unit cell, and the lateral arrangement is motivated by attractive, possibly hydrogen-bondlike, interactions between the oxygen containing anhydride groups and the hydrogen-terminated edges of the perylene cores of the PTCDA molecules. The packing is very similar to that of PTCDA in the [102] bulk plane.[22] On the contrary, after deposition at LT, i.e., below 150 K, a disordered metastable phase is formed. In this LT phase, the PTCDA molecules are arranged in small clusters of irregular shape and size, and as described in Ref.

7, the lateral intermolecular interactions are less well evolved, which causes that the electronic properties of the RT and LT phases are significantly different. Upon annealing the LT phase transforms irreversibly into the RT phase at about 170–200 K. As noted above, the details of the determination of the vertical bonding geometry of the PTCDA in the RT and LT adsorption state is the subject of the present paper.

II. EXPERIMENTAL PROCEDURE AND DATA EVALUATION

A. Experimental procedure

The data were collected during three beamtimes at the beamline ID 32 of the European Synchrotron Radiation Facility (ESRF) in Grenoble, France. A schematic of the experimental setup can be found in Ref. 21. Photoelectron spectra were taken with a hemispherical electron analyzer at an angle of θ=45° relative to the incoming x-ray beam. The photon energy was scanned stepwise over an energy interval around the Bragg condition of the Ag(111) surface, and photoelectron spectra were recorded for each photon energy. In some experiments, the photon energies were varied by larger steps further away from the maximum of the reflectivity curve, and by smaller steps close to the maximum in order to save measuring time (see, e.g., curves in Fig. 4). The photon flux is estimated at about 40 photons per PTCDA molecule and second.[20]

High pass energies (PE) of 47–58 eV were used for both the C 1*s* and O 1*s* spectra, if only integrated intensities of the photoemission lines were of interest. A small PE of 23 eV was used when good spectral resolution was required for the determination of the different chemical components within the O 1*s* spectra. Since the photoelectron yield for the investigated low *Z* element (C and O) is small, the data collection typically took several hours for each sample. In particular, measuring a set of O 1*s* spectra over the entire Bragg reflection range with high resolution took up to ~6 h.

The intensity of the reflected x-ray beam was monitored by the photoelectron current generated on a screen at a small angle close to the incoming x-ray beam. Prior to the data collection, the position of the x-ray beam on the clean sample was optimized in order to give the narrowest reflectivity curve, which typically had a half width of 0.85 eV.

The Ag(111) surface was prepared as described in Ref. 22. PTCDA was deposited onto the sample from a small home-built evaporator. For the preparation of the ordered RT phase the substrate was held at about 300 K. Monolayers were obtained by thermal desorption of the excess coverage.[24] For the preparation of the disordered LT phase, a substrate temperature of 100 K was used. These temperatures were also maintained during the data collection, which is essential for the LT phase, since it transforms irreversibly into the RT phase at temperatures above 170 K. For the latter experiment, a liquid He-cooled cryostat was used. The presence of the expected structural order and disorder of the RT and LT phase, respectively, were checked by low-energy electron diffraction. The absolute coverages were estimated by the intensity of the photoemission spectra, which were calibrated

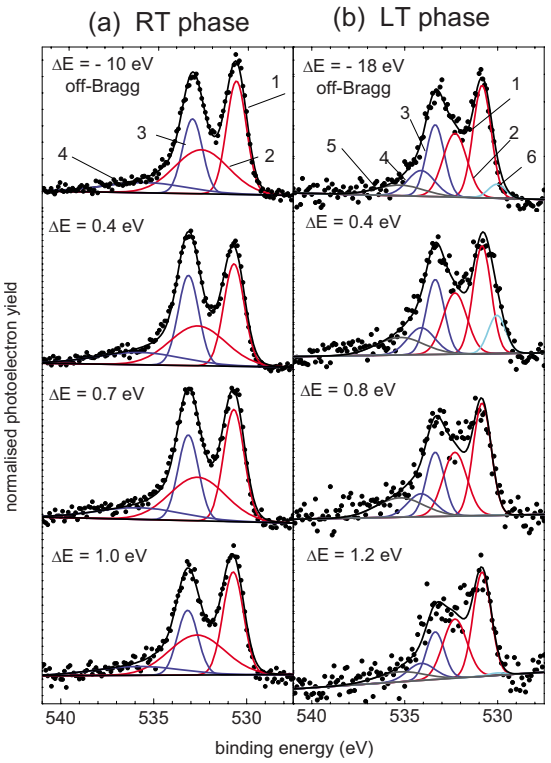

FIG. 1. (Color online) Photoemission (PE) spectra of the PTCDA O 1*s* level for (a) the RT phase and (b) the LT phase taken at a pass energy of 23 eV. The two spectra at the top were taken at off-Bragg photon energies and were used for the determination of the peak components (see text). The three spectra below were taken at photon energies close to the Bragg energy [$E_{\mathrm{Bragg}}^{\mathrm{exp}}$(RT phase) =2 633 eV and $E_{\mathrm{Bragg}}^{\mathrm{exp}}$ (LT phase at 100 K)=2 635 eV] and were used for the NIXSW analysis. $\Delta E = E_{\mathrm{photon}} - E_{\mathrm{Bragg}}$. The solid lines are fits to the experimental data on the basis of the indicated peak components. The peak components from the carboxylic oxygen are indicated in red, those of the anhydride oxygen in dark blue. A detailed description of all components is given in Table I. Experimental Bragg energies given here differ from nominal values due to ~3° off-normal incidence. Note that the binding energy scale in (a) has been slightly shifted with respect to that given in Ref. 6 due to an improved calibration.

to one monolayer (ML) of flat lying molecules in the ordered RT phase. For the LT phase we prepared coverages around 0.7 ML because we knew from earlier experiments that the phase slowly transforms into the RT phase if the coverage is too high, in particular, above 1 ML. Typical deposition rates were 0.1–0.2 ML per min.

B. Analysis of the photoemission spectra

1. General remarks

Figure 1 displays examples of O 1*s* photoelectron spectra for the RT and the LT phase of PTCDA on Ag(111). The two spectra in the top row were taken at photon energies far below the Bragg energy (off-Bragg spectra), where the geometric positions of the contributing atoms do not play a role due to the absence of the standing wave field. For both phases, the spectra show two dominant peaks. This occur-

rence of two peaks is related to the presence of two chemically different O species, namely, the *anhydride* and the *carboxylic* oxygen atoms in PTCDA. However, the two peaks do not simply correspond to the two contributing species, and the ratio of the respective peak areas is *not* 1:2, as expected from the stoichiometry, since, as we will describe in detail below, a satellite of the carboxylic oxygen also contributes to the anhydride peak at higher binding energies.[25] We note that for both phases, the photoemission averages over molecules on different adsorption sites since the respective differences are not resolved.

From the off-Bragg spectra it can be seen that the spectral line shapes differ for the RT and LT state. In particular, the valley between the two peaks is not as pronounced for the LT phase as for the RT phase. This difference is understandable in view of the different adsorption states of the molecules in the two phases. The three lower spectra in Fig. 1 are examples for spectra taken at photon energies which are a few tenths of an eV above the Bragg energy and for which the standing wave field has thus formed. The line shapes of these O 1*s* spectra change with energy which evidently demonstrates that the two types of O atoms must be on slightly different adsorption heights with respect to the Ag(111) substrate in both phases.

For the C 1*s* spectra, the spectral resolution was too low to resolve and separate the chemically different C species[26] seen in photoemission performed with higher resolution.[27] The direct comparison of the C 1*s* spectra of the RT and LT phases revealed very small differences in the line shapes (not shown), which are related to the different chemical bonding of the PTCDA to the Ag(111) surface in the two phases. Hence only the averaged C atom height could be determined from the integrated intensities of the C 1*s* spectra.

2. Fitting of different chemical components of oxygen

In order to determine the vertical positions of the carboxylic and anhydride O atoms separately, their respective contributions to the O 1*s* photoemission spectra had to be evaluated. For this purpose we performed fits to the spectra. Both the carboxylic and the anhydride oxygen were fitted by a doublet consisting of two Gaussian peaks (see Fig. 1). The positions and the full width at half maximum (FWHM) of the Gaussian peaks were determined from fits to the off-Bragg spectra. Two restrictions were made: (i) an area ratio of 2:1 for the two contributing doublets was required according to the stoichiometry and (ii) for the two dominant peaks (1 and 3) equal FWHM were used. In addition to the noted Gaussian peaks, a linear background was fitted. This description of the background was sufficient for the RT phase. For the LT phase, however, the background was found to be more structured. We modeled this by adding a broad Gaussian on the high binding energy side to the linear background [see Fig. 1(b), peak 5].

For the LT phase, the used fitting model was additionally justified by photoemission spectra which were measured with higher experimental resolution using a photon energy of 700 eV and a different electron analyzer.[28] After an appropriate background subtraction, positions and relative area ratios of the constituting peaks in these spectra were determined. They agree consistently with those peaks that fit the off-Bragg spectra shown here [see Fig. 1(b)]. However, one additional Gaussian peak had to be added on the low binding energy side of the spectrum to fit the present data [see Fig. 1(b), peak 6]. As shown below, the photon-energy-dependent absorption curve of this peak points to a significantly different bonding height compared to the so far considered peaks. Hence, we assume that this "spurious" peak originates from PTCDA molecules in an upright orientation, e.g., at island or step edges, as will be discussed below.

Table I summarizes the parameters of all Gaussian peaks and their respective physical origin. As seen from Fig. 1 and Table I, the peak positions and FWHM differ for the LT and RT phases, as it is expected from the different overall peak shapes. For both phases we obtain very good fits of the spectra at the off-Bragg condition and throughout the entire Bragg region. For these fits the positions of the peaks, their FWHM, and the ratios of the main peaks intensities to that of the respective satellites were kept constant. For alternative sets of Gaussians, the fits were of lower quality under the above restrictions and the coherent fractions of the resulting photoemission yield curves of the carboxylic and anhydride oxygen came out smaller. We hence had to conclude that these alternative fitting models do *not* separate the carboxylic and the anhydride oxygen correctly and hence dismissed them. In addition to the chemically resolved contributions to the O 1*s* spectra, we also computed the total area of the O 1*s* spectra after subtraction of a linear background, which yields the averaged height of the O atoms in the NIXSW analysis (see below).

3. Beam damage and adsorption of water over extended measuring times

Because of the long data-collection times and the hence extended exposure times of the sample to the x-ray beam, in particular, when the high-resolution O 1*s* spectra were collected, we carefully checked for time-dependent changes due to adsorption from the residual gas or any photochemical degeneration of the sample in both the photoemission spectra and the parameters determined from the NIXSW profiles. Here we comment only on the changes in the photoemission spectra, time-dependent changes in the coherent parameters will be discussed below.

Generally, no changes were found in the photoemission spectra, except for the measurements at low temperatures (100 K), where we found that water condensed on the surface with time when the sample was not exposed to the x-ray beam. This is illustrated in Fig. 2, where the O 1*s* spectrum (a) was measured on a "fresh," i.e., so far unexposed, spot on the sample and spectrum (b) after the spot had been exposed for 6 h. The H_2O adsorption has two effects on the O 1*s*-photoelectron spectra: first, a strong additional peak arises at a binding energy of 533 eV in good agreement with Ref. 29 and, second, the entire O 1*s*-spectrum shifts by about 1 eV to higher binding energies. We explain this peak shift by the interaction of the polar H_2O molecules and the anhydride groups of PTCDA. Such an interaction has been also observed in LT STM data,[30] and is very feasible, since the LT phase is disordered and exhibits void spaces between the

TABLE I. Overview on the Gaussian peaks used in the fit analysis of the O 1*s* photoemission spectra (see Fig. 1). The relative areas refer to the off-Bragg condition.

PTCDA/Ag(111)-RT Phase				
Peak no.	Binding energy (eV)	FWHM (eV)	Relative area (%)	Origin
1	530.67	1.30	33	Carboxylic O
2	530.67+1.95	3.53	34	Carboxylic O
3	530.67+2.45	1.30	21	Anhydride O
4	530.67+5.09	5.42	12	Anhydride O

PTCDA/Ag(111)-LT Phase				
Peak no.	Binding energy (eV)	FWHM (eV)	Relative area (%)	Origin
1	530.84	1.14	36	Carboxylic O
2	530.84+1.46	1.51	29	Carboxylic O
3	530.84+2.52	1.14	23	Anhydride O
4	530.84+3.28	1.72	12	Anhydride O
5	530.84+4.66	3.5		Background
6	530.84−0.80	1.1	4	unknown, noted as spurious (Not within the 100% given by the peaks 1–4)

PTCDA molecules.[7] Unfortunately, water cannot be thermally desorbed from the sample since higher temperatures cause the transformation of the metastable LT phase into the RT phase. However, we found that the intense x-ray beam (see Sec. II A) induces a selective photodesorption of water from the LT phase [spectrum (b)]. As a consequence the O 1*s* photoelectron electron spectra do not change with time due to water coadsorption, as long as the sample spot is continuously exposed to the x-ray beam. By maintaining the x-ray spot position on the sample during the measurements we hence could avoid the unwanted water contamination.

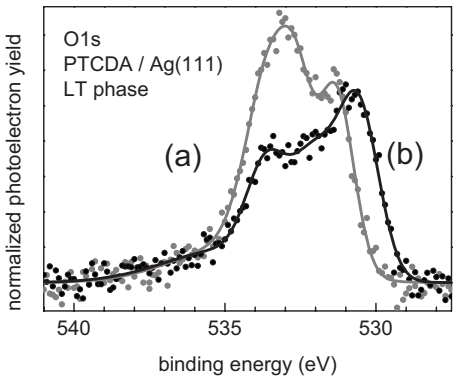

FIG. 2. Adsorption of water at low temperatures. O 1*s* photoemission spectra of the LT phase of PTCDA on Ag(111) for different times of exposure to the x-ray beam taken at a pass energy of 23 eV. (a) Fresh spot of a sample being held at low temperature for 11 h. (b) Same spot after 6 h exposure to the x-ray beam. The change in the peak shape is due to photon-induced desorption of water. The photon energy was about 17 eV below the Bragg condition.

C. Evaluation of the absorption curves and nondipolar corrections

1. General formula

The normalized photoelectron yield curves $I(E)$ can be described by[13]

$$I(E) = 1 + S_R R + 2|S_I|\sqrt{R} f_H \cos(\nu - 2\pi P_H + \Psi). \quad (1)$$

Herein the structural parameters f_H and P_H are the coherent fraction and coherent position related to the Bragg reflection with Miller indices "*H*" [here, $H=(111)$]. The photon-energy-dependent reflectivity is described by its amplitude R and ν, the phase of the standing wave. The parameters S_R and $S_I=|S_I|\exp(i\Psi)$ take account of higher-order contributions of the photoemission matrix element. In particular, they describe the effect that the momentum of the photon cannot be neglected, as in the dipole approximation, and that the photoelectrons are hence emitted with different directional distributions for the incoming and outgoing x-ray waves, respectively.[31] These nondipolar emission correction parameters S_R and S_I generally depend on the photon energy, the Z value of the emitting element, the orbital symmetry of the initial state, and the experimental geometry, i.e., the acceptance geometry of the electron detection and the direction and polarization of the photon beam. Within the dipole approximation S_R and S_I are equal to 1, however, for low-Z elements as C and O that are investigated here, and the photon energies used here, the nondipolar corrections are significant and have to be taken into account. For the backscattering geometry that we have employed (see above) the situation is as follows. The differential cross section for the emission of photoelectrons exited by the reflected (outgoing)

TABLE II. Overview on the nondipolar emission correction parameters used for the evaluation in this work. The values for Q were taken from Ref. 32, the values for Δ from Ref. 33. S_R, $|S_I|$, and Ψ were calculated according to Eq. (2).

	C 1*s*	O 1*s*
Q	0.31	0.31
Δ	−0.22	−0.33
S_R	1.900	1.900
$\|S_I\|$	1.453	1.457
Ψ	−0.069	−0.106

photons is higher compared to that excited by the incoming photons, leading to a value $|S_I|>1$ in Eq. (1). If instead $|S_I|=1$ is used, too large values of the coherent fractions f_H are fitted, compensating the too small $|S_I|$ value.

As described in Ref. 31, for our experimental geometry the parameters S_R, $|S_I|$, and Ψ are not independent but can be reduced to the two parameters Q and Δ by the following formulas:

$$S_R = (1+Q)/(1-Q), \quad |S_I| = (1+Q^2 \times \tan^2 \Delta)^{1/2}/(1-Q),$$

and

$$\tan \Psi = \tan \Delta (S_R - 1)/(S_R + 1). \tag{2}$$

For our analysis, we have used as input parameters Q values that were experimentally obtained[32] and Δ values which were theoretically compiled.[33] These values together with the computed values of S_R and $|S_I|$ are given in Table II. The phase difference Ψ was approximated by $\Psi \approx 0$. This approximation implies that the analysis of the photoelectron yield curves by Eq. (1) yields *effective* coherent positions $P_H = P_H^{true} + \Psi/2\pi$. However, for the used S_R and $|S_I|$ values, the estimated difference of the corresponding absolute coherent positions $[(d_{(111)}(P_H - P_H^{true})]$ is on the order of 0.03 and 0.04 Å for C and O, respectively, and is hence small.

Figures 3 and 4 display examples of normalized photoelectron yield curves derived from the C 1*s* spectra and O 1*s* spectra, respectively. For O 1*s*, both the total photoemission yield and the yields of the respective different chemical components are shown. The solid lines are fits to the curves on the basis of Eq. (1), using the nondipolar emission correction parameters summarized in Table II. For the determination of the structural parameters, we fitted several C 1*s* and O 1*s* yield curves by Eq. (1) individually. The fits were done with the program DARE.[34] In a second step, the averaged values of f_H and P_H were then computed from these results. These values are summarized in Table III. A two-dimensional representation of f_H and P_H in the form of the commonly used Argand diagram is given in Fig. 5.

From the averaged P_H values the absolute coherent positions were obtained as $d_H = (1+P_H)\ d_{(111)}$, using $d_{(111)}=2.3592$ Å (Ref. 35) at $T=300$ K, and $d_{(111)}=2.3503$ Å at $T=100$ K (Ref. 36) (see Table III). Strictly, the d_H values denote the distances with respect to the extended Ag(111) lattice planes. However, for PTCDA on the Ag(111) surface, the deviations of the surface Ag atoms

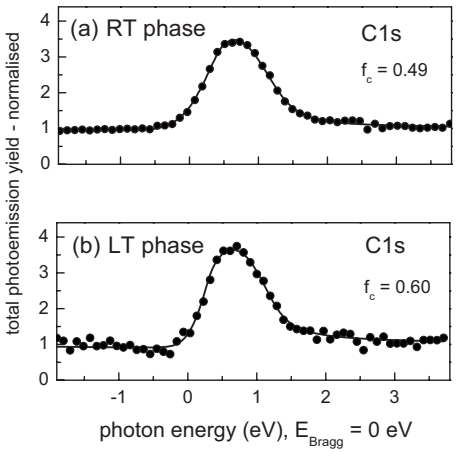

FIG. 3. Exemplary photoemission yield curves derived from C 1*s* spectra (measured at a pass energy of 47 eV) as a function of photon energy for (a) the RT phase and (b) the LT phase (symbols) and fits (solid lines) with respective coherent fractions f_C. Photon energies are measured relative to the respective Bragg energies.

from the extended (111) lattice plane due to a surface reconstruction are small. For the clean Ag(111) surface, this was experimentally verified.[37] For the PTCDA covered surface, the absence of a significant change in the first-layer distance due to the adsorption of PTCDA was derived from the analysis of the Ag Auger MVV emission as a function of photon energy. Since this signal stems from Ag atoms in the first layers, it would principally indicate the presence of a surface relaxation. However, the fits according to Eq. (1) yield the bulk lattice constant with a high coherent fraction of 0.86 ± 0.02 and 0.90 ± 0.03 at 300 and 100 K, respectively. Hence the coherent positions of C and O can be identified with the vertical adsorption heights of the specific atoms with respect to the top Ag(111) layer.

2. Discussion of the spurious peak

Figure 4 shows that the photoemission yield of the so-called spurious oxygen peak of the LT phase can be described well by Eq. (1), which indicates that this peak stems from a structurally well-defined chemical species. The coherent position P_H is found to amount to 0.65 ± 0.01, the corresponding f_H value is fitted to 1.0, but exhibits a large error due to the low statistics of this signal. The corresponding distance to the Ag surface is calculated in modulo $d_{(111)}$ to 1.54, 3.89, or 6.24 Å (± 0.03 Å). At present, we have no conclusive explanation for this peak. As reported above, coadsorbed H_2O leads to a peak at ~3 eV larger binding energies and can thus be ruled out. For CO adsorption from the residual gas, the sample temperature (100 K) was too high. Hence an origin due to PTCDA molecules which are either photochemically modified or adsorbed in unusual adsorption sites, e.g., in an upright position standing on the short or long edge of the molecule at island edges or steps edges may be possible. In this context we note that earlier STM investigations indeed found a step edge decoration on Ag(111) by PTCDA with an alternating vertical adsorption geometry of the PTCDA on the long and short axes along the

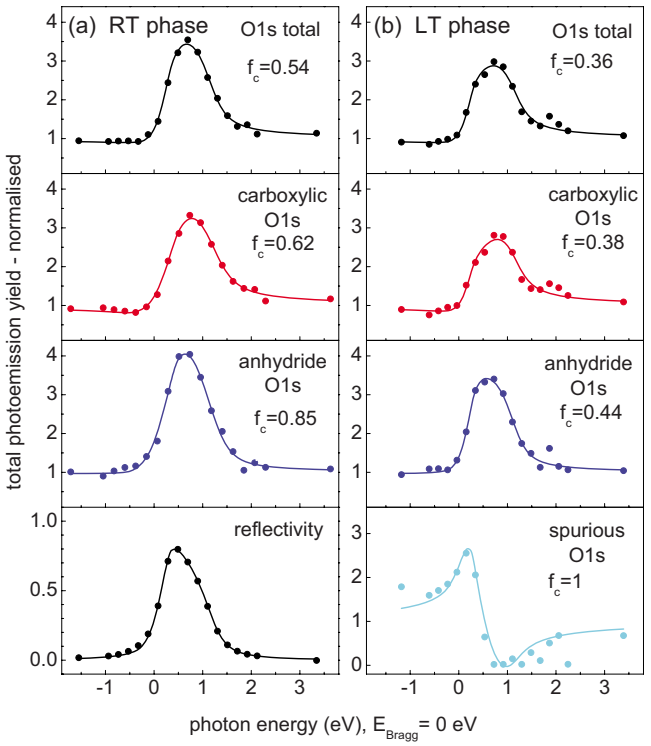

FIG. 4. (Color online) Exemplary set of photoemission yield curves derived from O 1*s* spectra (measured at a pass energy of 23 eV) as a function of photon energy for (a) the RT phase and (b) the LT phase (symbols) and fits (solid lines) with respective coherent fractions f_C. Photon energies are measured relative to the respective Bragg energies. From top to bottom: O 1*s* total intensity, intensity related to the carboxylic oxygen (red), intensity related to the anhydride oxygen (blue), reflectivity and the "spurious peak," respectively. The data points were taken on a nonequidistant grid for optimized data statistics. Fits were done according to Eq. (1) with a least-square fitting routine with equal weights of all data points. Photon energies are measured relative to the respective Bragg energies.

steps.[22] This latter model would be also compatible with the high coherent fraction (f_H=1.0) since the intermolecular distances between the different O atoms correspond roughly to $d_{(111)}$ and hence contribute constructively to f_H.

3. Systematic errors due to uncertainties in the nondipolar corrections

Prior to the discussion of the results, we consider some of the systematic uncertainties and difficulties of the evaluation. In principle, the accuracy of structural parameters determined by NIXSW is limited by several effects. First, the absolute values of the nondipolar emission parameters are known from theory and/or experiments with only limited accuracy at present. Second, the backward/forward asymmetry of the photoemission probability of atoms located on a surface may be modified (in addition to the influence of nondipolar effects) by back diffraction of the emitted photoelectrons from the underlying bulk into the direction of the analyzer. This photoelectron diffraction effect would mimic a higher effective Q value with respect to that based purely on the nondipolar emission corrections of the photoemission process. Finally, the subtraction of the substrate background for the determination of the photoelectron yields of the adsorbate is often a delicate task since this background is generally by two orders of magnitude larger compared to the photoemission signal of the adsorbate.

As noted above, the inclusion of the nondipolar emission correction parameters is important for the determination of the correct structural parameters. Unfortunately, the numerical values of these parameters that were determined by different experiments[32,33] and theoretical calculations[38] scatter within a certain range. For the *nominal* Bragg energies[39] of 2 627.7 eV (at 300 K) or 2 637.6 eV (at 100 K) of the present experiment and at θ=45°, Q values for C 1*s* between 0.24–0.37 have been reported,[17,18,21,32] while Q values for O 1*s* are between 0.26–0.34.[18,21,32,33,40] We used the values $Q_{C\,1s}$ =0.31 and $Q_{O\,1s}$=0.31.[32] The motivation for the choice of these values was twofold. First, these values were determined experimentally from incoherent layers of PTCDA on Ag(111) under the same experimental geometry as ours and may hence also include the effect of substrate back diffraction of photoelectrons, which is not accounted for by the theoretically determined Q values. Second, for these values, fits of the data by Eq. (1) yielded reasonable values for the coherent fractions of the adsorbate; in particular, the so obtained coherent fractions came out smaller than the coherent fractions that were fitted for the substrate, which is reasonable. For the second nondipolar emission correction parameter Δ, we used theoretically determined values, since experimental values are lacking.

Fortunately, the influence of the variation in Q on the fitted coherent position is not very large.[33] For our data we explicitly tested this by fitting the O 1*s* data (total intensity) for the above noted range of Q. The variation of $d^{O}_{(111)}$ was monotonic in Q and amounted to about 0.10 Å, for a variation Q=0.26–0.34, at the most.

4. Beam damage over long times

As noted above, differential changes in the photoemission spectra with increasing exposure time could not be detected. Nevertheless, we also monitored the long-time behavior of the coherent positions and fractions of the C 1*s* and the total O 1*s* signal (measured with low resolution) of the RT phase in order to check for possible variations in the structure of the adsorbate layer with time. For the C 1*s* signal we observed a small decrease of 4.7% (0.010) in the value of the coherent position (P_H) and of 18% (0.09) in the coherent fraction over a time of 24 h. The decrease in P_H causes only a small variation in the respective distance $[d_{(111)}(1+P_H)]$ by 1%, which is close to the statistical error. We interpret this result with a small amount of structural disorder that is induced by the x-ray beam.

For the O 1*s* signal, we further found small systematic differences in the coherent positions $d^{O}_{(111)}$ that were determined from the O 1*s* photoemission spectra measured with different spectral resolutions (PE). This coherent position $d^{O}_{(111)}$ corresponds to the averaged height of the two different O species (see Table III). In particular, we observed that $d^{O}_{(111)}$ values determined from spectra with *high resolution*

TABLE III. Values for the coherent positions and coherent fractions for the two phases of PTCDA on Ag(111) as obtained from the photoemission absorption profiles. The evaluation is based on Eq. (1) and includes the nondipolar corrections S_R and $|S_I|$ as described in the text. The phase Ψ was set to 0. The errors include only the statistical errors but not the systematic errors due to uncertainties in the nondipolar corrections or background subtraction. d_H was obtained as $(1+P_H)\, d_{(111)}$, using $d_{(111)}=2.3592$ Å at $T=300$ K and $d_{(111)}=2.3503$ Å at $T=100$ K. For the averaged values, photoemission yield curves computed from LR spectra taken at high pass energy were used (O 1*s* total in Fig. 4) while the values of the O components (carboxylic and anhydride) were computed from HR spectra taken at low pass energy. The second column notes the type and number of spectra which were evaluated. The given average values of $P_{(111)}$ and $f_{(111)}$ were calculated as $\frac{1}{N}\Sigma P_{(111),i}$ and $\frac{1}{N}\Sigma f_{(111),i}$ from the values determined from the individual spectra. For the carboxylic and anhydride O 1*s*, values which have been corrected by a 10% contribution of a bulklike signal ($P_H=0$) are given in brackets. For further details see text.

RT Phase

	Type, #	$P_{(111)}$	$d_{(111)}$ (Å)	$f_{(111)}$
C 1*s* averaged	LR, 8	0.214 ± 0.004	2.86 ± 0.01	0.54 ± 0.05
O 1*s* averaged	LR, 6	0.212 ± 0.010	2.86 ± 0.02	0.52 ± 0.06
O 1*s* carboxylic		0.128 ± 0.012	2.66 ± 0.03 [a]	0.47 ± 0.22
[corrected]	HR, 4	$[0.153 \pm 0.013]$	$[2.71 \pm 0.03]$	$[0.46 \pm 0.22]$
O 1*s* anhydride		0.263 ± 0.032	2.98 ± 0.08 [b]	0.79 ± 0.08
[corrected]	HR, 4	$[0.279 \pm 0.012]$	$[3.01 \pm 0.03]$	$[0.89 \pm 0.08]$

LT Phase

	Type, #	$P_{(111)}$	$d_{(111)}$ (Å)	$f_{(111)}$
C 1*s* averaged	LR, 3	0.193 ± 0.010	2.81 ± 0.02 [b]	0.62 ± 0.06
O 1*s* averaged	LR, 4	0.135 ± 0.009	2.67 ± 0.03	0.47 ± 0.05
O 1*s* carboxylic		0.063 ± 0.017	2.50 ± 0.04 [b]	0.40 ± 0.05
[corrected]	HR, 2	$[0.080 \pm 0.015]$	$[2.54 \pm 0.04]$	$[0.36 \pm 0.05]$
O 1*s* anhydride		0.204 ± 0.018	2.83 ± 0.04	0.48 ± 0.06
[corrected]	HR, 2	$[0.233 \pm 0.018]$	$[2.90 \pm 0.04]$	$[0.52 \pm 0.06]$

[a]Due to an improved statistics of the data this value is smaller by 0.02 Å compared to that given in Refs. 6 and 7.

[b]Likewise these values are by 0.01 Å larger.

(HR) (PE=23 eV) by direct evaluation of the total spectral area (for the RT phase) or by adding up the contributing components (i.e., the Argand vectors) of the O 1*s* spectrum (for the LT phase, avoiding the contribution of the spurious peak) (see Table I) came out systematically smaller by about 0.05 and 0.11 Å (for the RT and LT phase, respectively) compared to the values determined from spectra with *low resolution* (LR) (PE=47 eV). Principally, one would expect to obtain identical values from both types of spectra.

There are two possible explanations for this discrepancy. First, it may be possible that it is due to a small decrease in the quality of the adsorbate layer with time as discussed for the C 1*s* signal above. Notably the HR scans were preferentially taken *after* the LR scans, i.e., at higher sample age. Second, systematic errors in the subtraction of the photoelectron background (mainly due to the Ag) may play a role. Since the background is by orders of magnitude larger than the signal of the adsorbate even very minor systematic errors in the background subtraction can be relevant. As the background follows the Ag substrate signal, it corresponds to a component to the signal with a coherent position of $P_{(111)}=0$. Possibly very small differences in background subtraction exist between the LR and HR data.

By systematic testing we found that the averaged O 1*s* position from the HR data has to be corrected for an admixture of 10% by a coherent position of the substrate (e.g., $P^{Ag}_{(111)}=0$) to match the averaged O 1*s* position from the LR data. In the two-dimensional Argand diagram, such an admixture of the substrate can be visualized by vector addition.[12] So far we have no conclusive interpretation for this finding. The correction may be due to sample aging and a possible transfer of some of the PTCDA molecules to adsorption sites with a different vertical position with time. Alternatively, the noted differences in the background correction may play a role.

The values for the averaged O and the C positions in Table III are based on the LR scans. For the carboxylic and anhydride oxygen, the values directly derived from the HR

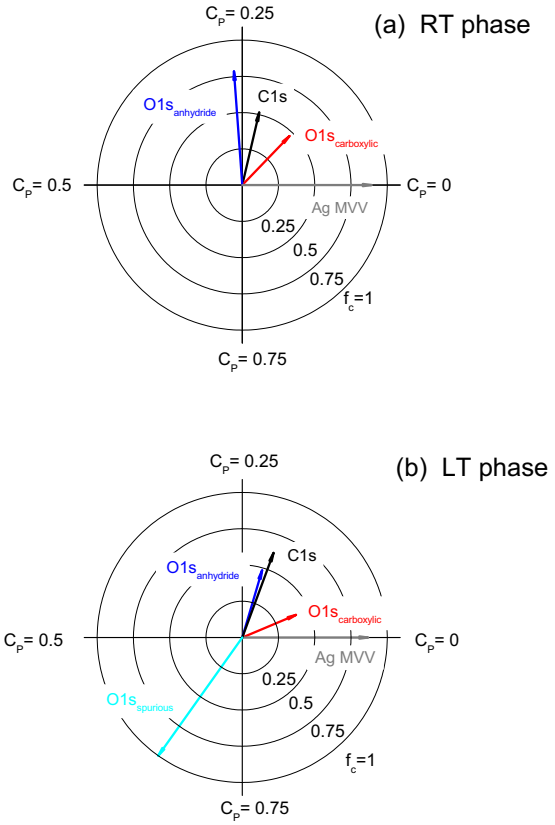

FIG. 5. (Color online) Argand diagrams of the averaged structural parameters determined for the two adsorption states of Table III: (a) RT phase and (b) LT phase. For further details see text.

scans are given. In addition, values corrected by a contribution of the substrate by 10%, as described above, are listed in Table III. Fortunately, these corrections are small and do not change the principal geometry of the two adsorbate species. Nevertheless, we mention this correction in order to stimulate other investigators to check on this issue and in order to indicate all possible errors.

III. RESULTS AND DISCUSSION

A. Molecular geometries

As noted above, Table III summarizes the structural parameters that were obtained for the two phases. Figure 6 illustrates the vertical distortions of both molecules that are derived from the obtained bonding distances. For the averaged C distance (d_C) we find 2.81 ± 0.02 Å and 2.86 ± 0.01 Å for the LT and RT phases, respectively. Hence the averaged carbon plane of PTCDA, which is mainly defined by the perylene core (containing 20 out of 24 C atoms), is closer by 0.05 Å to the Ag surface in the LT phase than in the RT phase. We note that this result is independent of the corrections by Ψ and the other nondipolar emission correction parameters. For both phases we further find that the carboxylic O atoms are located below the carbon plane whereas the anhydride O atoms are close to (LT phase) or above (RT phase) the carbon plane.

In both phases, the adsorption on the Ag(111) surface therefore causes a significant vertical distortion of the intrinsically planar PTCDA molecule. The difference in the vertical height of the two different types of O atoms, Δd_O, is of comparable size in both phases, i.e., 0.33 and 0.32 Å for the LT and RT phase, respectively. Hence we have a clear indication from the adsorption geometry that the PTCDA molecule is strongly bonded to the Ag(111) surface in both phases, because the gain in adsorption energy has to compensate the molecular distortion energy. This confirms the chemisorptive bonding of PTCDA on Ag(111) in both phases that was already derived on the basis of spectroscopic data.[41,42]

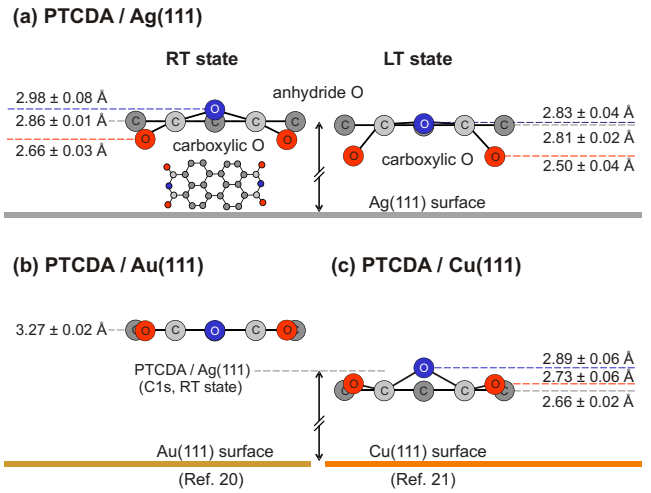

FIG. 6. (Color online) Hard sphere models of PTCDA/Ag(111) for the RT state and LT state, respectively. For comparison, models for PTCDA on Au(111) (Ref. 20) and Cu(111) (Ref. 21) are given. Note that on Au(111), the O positions could not be determined due to experimental reasons. The vertical length scale is expanded by a factor of 3. Red/blue circles: carboxylic/anhydride O atoms; light/dark gray circles: C atoms in anhydride groups/perylene core. The molecule is viewed along its long axis. The inset illustrates the structure of the PTCDA molecule.

The coherent fractions of the C 1*s* signals (f^C) of both phases are in an intermediate range (0.62 and 0.54 for the LT and RT phase, respectively), which is rather typical for adsorbates of this type.[18,21] Several reasons that cause a reduction in the coherent fractions can be discussed. A structural (saddlelike) distortion of the perylene core, due the downward bonding of the carboxylic O atoms, as indicated by density-functional theory (DFT) calculations,[3,8] may play a role. However, this effect on f^C is small, below 10%. This can be estimated from the vertical splitting Δd_O of the positions of the different types of O atoms (0.33 and 0.32 Å), which sets a reasonable upper limit for the perylene core distortion. The difference in the adsorption heights of the two inequivalent molecules per unit cell in the RT phase, which is estimated at 0.06 Å from DFT calculations,[3] may principally also contribute, but is definitely too small to cause a relevant effect on the coherent fractions. A small effect may further be due to Ag lattice vibrations which cause a smaller reflectivity by a reduced Debye-Waller factor. This was so far not accounted for in the fits of the photoemission yield curves by Eq. (1). From calculations using an alternative evaluation code[43] we estimate this effect to be on the order of

20% for the RT phase and less than 5% for the LT phase. Therefore, other effects must be also responsible for the reduction in the coherent fractions f_H. One is most likely the effect due to static disorder, which yields a small admixture to the signal from the PTCDA molecules at defect sites with different adsorption heights, as noted above. The other effect would be that the dipolar corrections are overestimated, i.e., in particular the $|S_I|$ values in Eq. (1) are too large, which is compensated by too small values of f_H.

The smaller bonding distance d_C of the disordered LT state with respect to the RT state is remarkable and points to a different bonding of the two states to the Ag(111) surface. This difference in the two states can be also seen from differences in their respective valence band spectra [ultraviolet photoemission spectroscopy (UPS) and scanning tunneling spectroscopy (STS)].[7] This difference can be interpreted with a modification of the bonding of the carboxylic O atoms to the Ag surface. In the disordered LT state, this bond is rather strong and is less affected by nearest-neighbor PTCDA molecules; in the ordered and densely packed RT state, however, lateral interactions between these carboxylic O atoms and H atoms on neighboring PTCDA molecules form and compete with the vertical O-Ag bonds. This competition *weakens* the O-Ag bond by likely several direct and indirect effects as will be discussed in more detail below. As a consequence the bonding of the entire molecule to the Ag(111) surface is modified and the vertical bonding distance of the perylene core increases in the ordered RT phase.

B. Bonding mechanisms of PTCDA to Ag(111)

Initially, the bonding of PTCDA to the Ag(111) surface was mainly discussed in relation to the partial filling of the *former* lowest unoccupied molecular orbital (FLUMO) upon overlap with s/p-type states of the Ag(111) surface.[22,44] The most prominent consequence is a strong enhancement of in-plane Raman modes by dynamical interfacial charge transfer from the s/p states in and out of the FLUMO which is seen for the RT phase.[44] The role of the carboxylic O atoms for the bonding was recognized only more recently, when the molecular distortion described above was found.[6]

The bonding via the carboxylic O atoms was also deduced from DFT calculations of PTCDA/Ag(111) by Ji *et al.*[4] Evidently, a separation of these two different bonding channels (perylene core/carboxylic O) is not very reasonable, if not impossible, since they mutually support each other, as discussed in Refs. 3, 4, and 6. This can possibly be also inferred from the comparison with the ordered commensurate phase of the smaller NTCDA molecule. NTCDA on Ag(111) exhibits an about 5% larger vertical bonding distance (d_C) than PTCDA (see Table IV).[18] Since NTCDA exhibits the identical anhydride groups as PTCDA, its smaller core (naphthalene instead of perylene) appears to be responsible for the difference at first glance. However, differences in the lateral arrangement of NTCDA with respect to PTCDA may principally also be important here. Namely, in the ordered NTCDA monolayer, the anhydride groups are directly facing each other,[45] and hence the accumulation of negative partial charges on these may be suppressed, hence reducing the overall polarization of the molecule and in particular of the core, causing the larger vertical bonding distance compared to PTCDA/Ag(111).

TABLE IV. Values for the averaged vertical distances d_C of the carbon and d_O of the O atoms for PTCDA and NTCDA adsorbed on different (111) metal surfaces. Δd_O notes the difference in the vertical distance of the carboxylic and anhydride oxygen positions (the vertical splitting). For PTCDA/Au(111) the O position was not measured for experimental reasons (Ref. 20). Note that for PTCDA/Cu(111), contrary to all other cases, both the carboxylic *and* the anhydride oxygen are above the averaged C height.

	d_C (Å)	d_O (Å)	Δd_O (Å)
PTCDA			
PTCDA/Au(111)[a]	3.27 ± 0.02		
RT-PTCDA/Ag(111)	2.86 ± 0.01	2.86 ± 0.02	0.32 ± 0.11
LT-PTCDA/Ag(111)	2.81 ± 0.02	2.67 ± 0.03	0.33 ± 0.08
PTCDA/Cu(111)[b]	2.66 ± 0.02	2.81 ± 0.03	0.16 ± 0.08
NTCDA			
NTCDA/Ag(111)[c]	3.00 ± 0.02	2.87 ± 0.01	0.26 ± 0.04

[a]Reference 20.
[b]Reference 21.
[c]Reference 18.

Concerning the involved Ag states, both s/p- and d-band states appear to be relevant. The importance of the d-band bonding was argued, e.g., on the basis of the observed vacuum level shifts for PTCDA monolayers on Ag, Au, and Cu by Kawabe *et al.*[46] We will come back to this point below, when we compare the bonding distances of PTCDA on different metals. In addition to these chemical bonds between PTCDA and the Ag surface, van der Waals (vdW) bonds between PTCDA and the Ag surface are relevant. This is for instance conjectured from the observation that DFT calculations (using different functionals, local-density approximation, and generalized gradient approximation) are not able to correctly model the observed bonding distance of the molecule.[3] The discrepancy results from the insufficient account of the vdW interactions by DFT;[5] in reverse, it thus highlights the important role of the vdW interactions for the bonding of these larger organic molecules to metal surfaces.

Besides the above noted (vertical) molecule/metal interactions, intermolecular (lateral) interactions are also relevant for the vertical adsorption geometry of the PTCDA molecule on Ag(111), as demonstrated by the reported differences between the two phases. This effect is remarkable since it reveals the high complexity of the metal/adsorbate bond in this system and points to the competition between the lateral and vertical bonding channels. Different components in the lateral molecule-molecule interactions may be relevant. First of all, hydrogenlike attractive lateral interactions between the carboxylic O atoms and H atoms on the periphery of the perylene core of a next-neighbor molecule can be expected from the herringbone arrangement of the PTCDA molecules in the monolayer. The length of the distances between car-

boxylic O atoms and hydrogen atoms are 2.04–2.55 Å (Ref. 23) and are hence well in the range of hydrogen bonds.[47] As a direct consequence the H atoms exert an upward directed force on the O atoms which compete with the O-Ag bonds. Furthermore, a charge transfer related to this bond, namely, the donation of charge from the carboxylic O atoms to the H atoms, could play a role. It reduces the charge that is otherwise available to form the O-Ag bonds and hence weakens the vertical bond of the carboxylic O to the Ag surface. In addition to these more direct interactions between PTCDA molecules, a metal-mediated interaction component may play a role: Upon adsorption of an *ordered* PTCDA layer, the Shockley surface state of the Ag(111) surface is depopulated and shifted upward by 0.6 eV, whereby it gets in resonance with unoccupied states (mainly LUMO+1) of the molecule and forms an interface state with strong metallic character above the Fermi level.[10,48] This state is strongly delocalized and was imaged by STM.[49] The effect reduces the s/p band density of states and hence could also weaken the PTCDA bond to the s/p band, in agreement with the experimental finding for the RT phase. Finally, the intermolecular bonding and the concomitant change of the O-Ag bond may have a back action on the central bond of the perylene core to the Ag. Namely, a smaller polarization of the perylene core due to smaller partial charges on the carboxylic O atoms in the RT phase could be relevant and additionally weaken the bond of the perylene core to the Ag surface.

C. Comparison with other surfaces

It is interesting to compare the obtained adsorption geometries of PTCDA on Ag(111) to those for PTCDA on Au(111) (Ref. 20) and Cu(111).[21] As can be seen in Table III and as illustrated in Fig. 6, the averaged C bonding distance d_C, increases systematically from Cu via Ag to Au. The difference between d_C on Cu(111) and Au(111) amounts to 0.61 Å. Unfortunately, the position of the O atoms could not be measured for PTCDA on Au(111) due to experimental reasons,[20] which hence excludes a systematic comparison of the O positions and their splitting. However, we note that for PTCDA/Cu(111), the vertical displacement pattern of the O atoms is principally different from that found for PTCDA/Ag(111), namely, both types of O atoms are at larger distances than d_C (see Fig. 6). This might indicate that the bond of the carboxylic O to the metal, present for PTCDA/Ag(111), does not form for PTCDA/Cu(111), but that a stronger localized bond of the carboxylic C to the Cu(111) surface, possibly leading to a an sp^3 configuration of the C atom, exists.

From the bonding distances (d_C), PTCDA/Au(111) can be well described as a *physisorbed* system,[20] whereas PTCDA/Ag(111) and Cu(111) have to be considered as *chemisorbed* systems. This assignment is also supported by the changes in the frontier orbitals due to the bonding as seen in UPS.[42] Duhm *et al.*[50] have already pointed out the correlation of the occupancy of the former LUMO and the adsorption height of PTCDA on Cu(111), Ag(111), and Au(111). On Cu(111), a LUMO-derived molecular hybride state (FLUMO) is formed 0.8 eV below the Fermi energy (E_F). On Ag(111), a partially filled LUMO derived state is found at the Fermi edge, while on Au(111), no LUMO derived state is found below E_F, which is interpreted with the fact that the LUMO does not mix with metallic states and is hence left unoccupied. These observations can be summarized under the aspect that charge transfer into the FLUMO increases from Au via Ag to Cu. However, as noted by Kawabe *et al.*,[46] the interfacial dipole, which can be monitored by the change in the work function $\Delta\phi$ upon absorption of the monolayer, cannot be understood by a simple charge-transfer model between delocalized s/p metal states and molecular states. This is taken as an evidence for the relevance of hybridization of the molecular states with lower lying d-band metal states.[46]

In the context of the adsorption heights, the following correlation appears to us to be of interest, namely, that between the adsorption heights (d_C), which are corrected for the different sizes of the surface atoms, and the work functions of the bare surfaces. For this purpose we calculated the adsorption height d_C^{vdW} above the vdW spheres of the surface atoms

$$d_C^{vdW} = d_C - r_{vdW}^{substrate}. \tag{3}$$

This correction in particular accounts for the smaller vdW radius of Cu as compared to the vdW radii of Ag and Au. We used $r_{vdW}^{Cu}=1.40$ Å, $r_{vdW}^{Ag}=1.72$ Å, and $r_{vdW}^{Au}=1.66$ Å.[51] Alternatively, one could have also corrected for the covalent radii, which gives similar results, since these differ not much from the vdW radii.[20] We can expect that d_C^{vdW} describes the distance of the perylene core above the "cut-off edge" of the substrate electron density in good approximation. Here we refer only to the ordered RT phase of PTCDA/Ag(111) since on Cu(111) (Ref. 52) and Au(111) (Ref. 20) only ordered phases of PTCDA at RT were investigated. The d_C^{vdW} values are plotted versus ϕ in Fig. 7. The values for ϕ of the clean surfaces were taken from Ref. 53. Remarkably, the correlation of d_C^{vdW} and ϕ is linear within very good approximation. If PTCDA were physisorbed on all three surfaces, d_C^{vdW} would be approximately constant and match the vdW radius r_{vdW}^C of carbon. For perylene the respective value is $r_{vdW}^C=1.75$ Å (Ref. 51) which is close to the bonding distance observed on Au(111). We note that the linear correlation of Fig. 7 would not be obtained if the d_C values were not corrected by Eq. (3). In that case, the Cu(111) surface would have the smallest bonding distance whereas we find it for Ag(111).

Of course the obtained correlation is so far only an experimental observation and further conclusions should be considered with care, in particular, because of the small number of data points. However, it is interesting to discuss this correlation under the aspect of the bonding mechanism. The observed correlation of d_C^{vdW} and ϕ expresses that the bonding distance of the perylene core to the substrate electron density decreases with smaller values of ϕ. As noted above, electron donation from the substrate into the LUMO of PTCDA, which is mainly localized on the perylene core, is relevant for the bonding distance. Bonding by charge transfer into unoccupied molecular levels has been considered within the Anderson-Newns model.[54,55] This model has been, in particular, used to describe the interaction of s/p substrate states

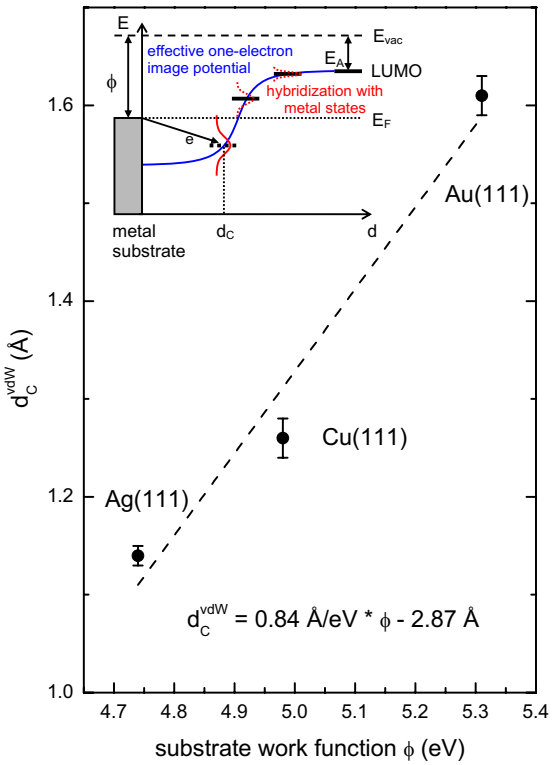

FIG. 7. (Color online) Vertical bonding distances d_C^{vdW} of PTCDA corrected by the van der Waals radii (r_{vdW}) of the surface atoms versus workfunctions ϕ on different (111) coinage metal surfaces ($d_C^{vdW}=d_C-r_{vdW}$). The correction by r_{vdW} accounts for differences in the atomic sizes (Ref. 51). For the d_C values of PTCDA/Cu(111) and PTCDA/Au(111) see Refs. 21 and 20, respectively. Work functions of the clean metals are from Ref. 53. The dashed line represents a linear fit to the data points. The empirically found correlation between d_C^{vdW} and ϕ is given. The inset illustrates schematically the energetic lowering and occupation by electrons of the LUMO and is discussed in the text.

with molecules. The underlying principle is illustrated in the inset of Fig. 7. In a first step, the approach of the molecule to the metal surface leads to broadening and energetic lowering of the LUMO due to interaction with the metal states, in particular, with the respective image states. Population of the former LUMO occurs, when the orbital falls below the Fermi energy E_F. In a second step, the interaction of the so formed molecule—metal hybride states with d states of the substrate is considered.

The position of the LUMO with respect to E_F for the molecule at a large distance to the surface is expected to be at ϕ-E_A where E_A denotes the affinity level of PTCDA, i.e., $E_A=E_{vac}-E_{LUMO}$ (see Fig. 7, inset). Within this model, smaller values of ϕ bring the LUMO, mainly located on the perylene core, closer to E_F and evidently cause an earlier occupation of the LUMO, i.e., at a larger molecule surface distance. As a consequence the related bonding is stronger and hence pulls the molecule closer to the surface as seen by the decrease in d_C^{vdW}. Within this model, the work function of the bare metal surface constitutes the *primary* control parameter for the bonding distance.

Hybridization with metal d states, possibly involving mainly the carboxylic O containing groups, appears to contribute only in *second* order to the bonding distance. The resulting order of the bonding distances d_C^{vdW} is different to what is observed for the hybridization and the resulting energetic position of, e.g., the FLUMO. Namely, the binding energy of the FLUMO of PTCDA on Cu(111) is found to be −0.8 eV (peak L'' in Ref. 50) and to be the smallest among the considered substrates. [On Ag(111) the broad FLUMO is located at the Fermi edge and partially filled while on Au(111) it is above the Fermi energy and empty.] This strong downward shift of the FLUMO on Cu is likely related to the energetic position of the d states of Cu(111), which are at about 2 eV higher binding energy compared to Ag(111) and Au(111),[50] and which hence can strongly interact with the PTCDA orbitals. Remarkably, this interaction does not further reduce the bonding distance. Hence the electronic modification of the orbital system of the adsorbate and the bonding distance are possibly controlled by different aspects of the substrate. While the s/p states are responsible for the bonding distance, the d-band states induce the final hybridization and binding energy. We finally note that the above described model so far neglects the specific role of the carboxylic O atoms for the bonding, which might be different in the three systems. Evidently this model is speculative at present, however, it could be experimentally tested on other comparable systems.

IV. SUMMARY

For PTCDA adsorbed on the Ag(111) surface, the vertical distances in the disordered low-temperature phase and the ordered room-temperature phase are found to be different. In particular, the averaged vertical bonding distances of the C and O atoms are smaller for the LT phase compared to the RT phase, which is explained by a weakening of the PTCDA Ag bond by competitive intermolecular interactions in the ordered RT phase and a possible back action of this on the bond of the perylene core to the Ag(111) surface. Concerning the averaged bonding distance of the C atoms, the values of these two phases are found to be in between the values that were determined for PTCDA on the Au(111) and the Cu(111) surface. In comparison with the latter two surfaces, we find an interesting correlation of the bonding height of the PTCDA above the van der Waals spheres of the substrate atoms with the work function of the bare surface.

ACKNOWLEDGMENTS

We thank A. Gerlach, C. Kumpf, F. Schreiber, C. Stadler, C. Schalley, E. Umbach, and W. Moritz for helpful discussions and experimental support, J. Zegenhagen for providing the program DARE. Support by the ESRF and the DFG under the Projects No. SFB 624, No. SO-407, and No. TA-244 is acknowledged.

*Also at Jacobs University, School of Engineering and Science, P.O. Box 750761, 28725 Bremen, Germany.
†Corresponding author. FAX: +49 (0)228-73 2551; sokolowski@pc.uni-bonn.de

[1] *Organic Electronics*, edited by H. Klauk (Wiley-VCH, Weinheim, 2006).
[2] A. Alkauskas, A. Baratoff, and C. Bruder, Phys. Rev. B **73**, 165408 (2006).
[3] M. Rohlfing, R. Temirov, and F. S. Tautz, Phys. Rev. B **76**, 115421 (2007).
[4] W. Ji, Z.-Y. Lu, and H.-J. Gao, Phys. Rev. B **77**, 113406 (2008).
[5] M. Rohlfing and T. Bredow, Phys. Rev. Lett. **101**, 266106 (2008).
[6] A. Hauschild, K. Karki, B. C. C. Cowie, M. Rohlfing, F. S. Tautz, and M. Sokolowski, Phys. Rev. Lett. **94**, 036106 (2005).
[7] L. Kilian, A. Hauschild, R. Temirov, S. Soubatch, A. Schöll, A. Bendounan, F. Reinert, T.-L. Lee, F. S. Tautz, M. Sokolowski, and E. Umbach, Phys. Rev. Lett. **100**, 136103 (2008).
[8] R. Rurali, N. Lorente, and P. Ordejon, Phys. Rev. Lett. **95**, 209601 (2005).
[9] A. Hauschild, K. Karki, B. C. C. Cowie, M. Rohlfing, F. S. Tautz, and M. Sokolowski, Phys. Rev. Lett. **95**, 209602 (2005).
[10] F. S. Tautz, Prog. Surf. Sci. **82**, 479 (2007).
[11] J. Zegenhagen, Surf. Sci. Rep. **18**, 199 (1993).
[12] D. P. Woodruff, Prog. Surf. Sci. **57**, 1 (1998).
[13] D. P. Woodruff, Prog Phys. **68**, 743 (2005).
[14] R. G. Jones, A. S. Y. Chan, M. G. Roper, M. P. Skegg, I. G. Shuttleworth, C. J. Fisher, G. J. Jackson, J. J. Lee, D. P. Woodruff, N. K. Singh, and B. C. C. Cowie, J. Phys.: Condens. Matter **14**, 4059 (2002).
[15] L. Kilian, W. Weigand, E. Umbach, A. Langner, M. Sokolowski, H. L. Meyerheim, H. Maltor, B. C. C. Cowie, T. Lee, and P. Bäuerle, Phys. Rev. B **66**, 075412 (2002).
[16] A. Gerlach, F. Schreiber, S. Sellner, H. Dosch, I. A. Vartanyants, B. C. C. Cowie, T. L. Lee, and J. Zegenhagen, Phys. Rev. B **71**, 205425 (2005).
[17] C. Stadler, S. Hansen, F. Pollinger, C. Kumpf, E. Umbach, T. L. Lee, and J. Zegenhagen, Phys. Rev. B **74**, 035404 (2006).
[18] C. Stadler, S. Hansen, A. Schöll, T. L. Lee, J. Zegenhagen, C. Kumpf, and E. Umbach, New J. Phys. **9**, 50 (2007).
[19] C. Stadler, S. Hansen, I. Kröger, C. Kumpf, and E. Umbach, Nat. Phys. **5**, 153 (2009).
[20] S. K. M. Henze, O. Bauer, M. Sokolowski, and S. Tautz, Surf. Sci. **601**, 1566 (2007).
[21] A. Gerlach, S. Sellner, F. Schreiber, N. Koch, and J. Zegenhagen, Phys. Rev. B **75**, 045401 (2007).
[22] K. Glöckler, C. Seidel, A. Soukopp, M. Sokolowski, E. Umbach, M. Böhringer, R. Berndt, and W.-D. Schneider, Surf. Sci. **405**, 1 (1998).
[23] A. Kraft, R. Temirov, S. K. M. Henze, S. Soubatch, M. Rohlfing, and F. S. Tautz, Phys. Rev. B **74**, 041402(R) (2006).
[24] L. Kilian, E. Umbach, and M. Sokolowski, Surf. Sci. **573**, 359 (2004).
[25] P. J. Unwin, D. Onoufriou, and T. S. Jones, Surf. Sci. **547**, 45 (2003).
[26] A. Hauschild, Ph.D. thesis, University of Bonn, 2007.
[27] A. Schöll, Ph.D. thesis, University of Würzburg, 2003.
[28] A. Schöll (private communication).
[29] A. F. Carley, P. R. Davies, M. W. Roberts, and K. K. Thomas, Surf. Sci. Lett. **238**, L467 (1990).
[30] R. Temirov and F. S. Tautz (private communication).
[31] D. P. Woodruff, Nucl. Instrum. Methods Phys. Res. A **547**, 187 (2005).
[32] F. Schreiber, K. A. Ritley, I. A. Vartanyants, H. Dosch, J. Zegenhagen, and B. C. C. Cowie, Surf. Sci. **486**, L519 (2001).
[33] J. J. Lee, C. J. Fisher, D. P. Woodruff, M. G. Roper, R. G. Jones, and B. C. C. Cowie, Surf. Sci. **494**, 166 (2001).
[34] J. Zegenhagen, 2002, the program DARE calculates the theoretical total PE yield on the basis of dynamical x-ray scattering theory.
[35] P. Eckerlin and H. Kandler, *Landolt-Börnstein* (Springer-Verlag, Berlin, 1971).
[36] N. W. Ashcroft and N. D. Mermin, *Solid State Physics* (Hartcourt College Publishers, Philadelphia, 1975).
[37] E. A. Soares, V. B. Nascimento, V. E. de Carvalho, C. M. C. de Castilho, A. V. de Carvalho, R. Toomes, and D. P. Woodruff, Surf. Sci. **419**, 89 (1999).
[38] T. Fujikawa, R. Suzuki, A. Hiroko, H. Shinotsuka, and L. Köver, J. Electron Spectrosc. Relat. Phenom. **159**, 14 (2007).
[39] These Bragg energies are calculated for a Bragg angle of 90°.
[40] J. Stanzel, W. Weigand, L. Kilian, H. L. Meyerheim, C. Kumpf, and E. Umbach, Surf. Sci. **571**, L311 (2004).
[41] M. Jung, U. Baston, G. Schnitzler, M. Kaiser, J. Papst, T. Porwol, H. J. Freund, and E. Umbach, J. Mol. Struct. **293**, 239 (1993).
[42] Y. Zou, L. Kilian, A. Schöll, T. Schmidt, R. Fink, and E. Umbach, Surf. Sci. **600**, 1240 (2006).
[43] O. Bauer *et al.*, *XSWAVES - An XSW Data Evaluation Routine for ORIGIN 8* (University of Bonn, Bonn, 2009).
[44] M. Eremtchenko, J. A. Schaefer, and F. S. Tautz, Nature (London) **425**, 602 (2003).
[45] L. Kilian, U. Stahl, J. Kossev, M. Sokolowski, R. Fink, and E. Umbach, Surf. Sci. **602**, 2427 (2008).
[46] E. Kawabe, H. Yamane, R. Sumii, K. Koizumi, Y. Ouchi, K. Seki, and K. Kanai, Org. Electron. **9**, 783 (2008).
[47] T. Steiner, Angew. Chem., Int. Ed. **41**, 48 (2002).
[48] C. H. Schwalb, S. Sachs, M. Marks, A. Schöll, F. Reinert, E. Umbach, and U. Höfer, Phys. Rev. Lett. **101**, 146801 (2008).
[49] R. Temirov, S. Soubatch, A. Luican, and F. S. Tautz, Nature (London) **444**, 350 (2006).
[50] S. Duhm, A. Gerlach, I. Salzmann, B. Broker, R. L. Johnson, F. Schreiber, and N. Koch, Org. Electron. **9**, 111 (2008).
[51] A. Bondi, J. Phys. Chem. **68**, 441 (1964).
[52] T. Wagner, A. Bannani, C. Bobisch, H. Karacuban, and R. Möller, J. Phys.: Condens. Matter **19**, 056009 (2007).
[53] H. B. Michaelson, J. Appl. Phys. **48**, 4729 (1977).
[54] D. M. Newns, Phys. Rev. **178**, 1123 (1969).
[55] J. K. Norskov, Rep. Prog. Phys. **53**, 1253 (1990).